

Velocity Field: An Informative Traveling Cost Representation for Trajectory Planning

Ren Xin^{1,2}, Jie Cheng², Sheng Wang^{1,2} and Ming Liu^{1,2,3}

Abstract—Trajectory planning involves generating a series of space points to be followed in the near future. However, due to the complex and uncertain nature of the driving environment, it is impractical for autonomous vehicles (AVs) to exhaustively design planning rules for optimizing future trajectories. To address this issue, we propose a local map representation method called *Velocity Field*. This approach provides heading and velocity priors for trajectory planning tasks, simplifying the planning process in complex urban driving scenarios. The heading and velocity priors can be learned from demonstrations of human drivers using our proposed loss functions. Additionally, we developed an iterative sampling-based planner to train and compare the differences between local map representation methods. We investigated local map representation forms for planning performance on a real-world dataset. Compared to learned rasterized cost maps, our method demonstrated greater reliability and computational efficiency.

The video can be found at <https://youtu.be/5LuyGN58CD0>.

I. INTRODUCTION

Trajectory planning is an essential component of autonomous driving systems [1], as it makes the vehicle follow a target path to the intended destination with the promise of efficiency and safety. Existing planning methods can be classified into two categories: rule-based methods and learning-based methods.

Rule-based methods rely on manually designed rules to avoid collisions with objects in the driving context, such as distance measurement and velocity strategy based on distance, as shown in Fig. 1 (a). However, these rules are often limited to specific scenarios, thus restricting their generalization ability. Learning-based methods, particularly those based on imitation learning, learn the mapping between trajectory and driving context, providing a broader range of applications. Nevertheless, directly mapping driving context to planning trajectory is often considered poorly interpretable [2].

The Neural Motion Planner (NMP) [2] introduced a novel approach that integrates the benefits of rule-based and learning-based methods, thereby improving the generalization and interpretability of the planning module. Specifically,

This work was supported by Guangdong Basic and Applied Basic Research Foundation, under project 2021B1515120032, National Natural Science Foundation of China under Grants 62333017, and Project of Hetao Shenzhen-Hong Kong Science and Technology Innovation Cooperation Zone(HZQB-KCZYB-2020083), awarded to Prof. Ming Liu. (Corresponding author: Ming Liu.)

¹The Hong Kong University of Science and Technology (Guangzhou), Nansha, Guangzhou, 511400, Guangdong, China. ²The Hong Kong University of Science and Technology, Hong Kong SAR, China. ³HKUST Shenzhen-Hong Kong Collaborative Innovation Research Institute, Futian, Shenzhen, China. (Email: {rxin, jchengai, swangei}@connect.ust.hk, eelium@ust.hk).

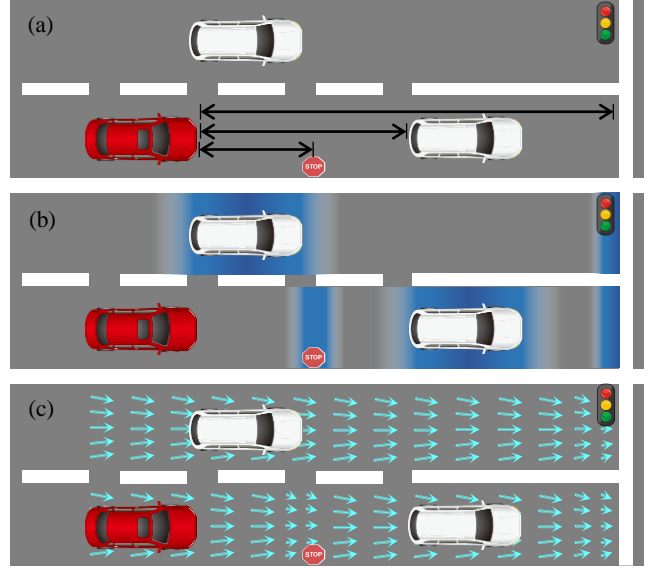


Fig. 1. This figure illustrates three methods for calculating the cost of travel at a given time step. The red car represents the ego vehicle, the solid white line on the far right depicts the stop line for the traffic light, and the traffic lights in each scenario are in the red light state. (a) distances between the ego vehicle and other vehicles and traffic signals are measured. Manually defined rules are then implemented to determine the car-following speed and lane change maneuvers. (b) represents a class of map representations that provide the driving cost for each point in the driving context. It guides the vehicle trajectory through as many low-driving cost areas as possible. (c) uses the velocity vector to guide the vehicle's driving trajectory. For example, it instructs vehicles to slow down and stop before the stop line around stop signs and to drive at the same speed as other cars.

this method employs a deep neural network to convert perceptual information into driving cost at each space-time point in the scenario (Fig. 1 (b)), and selects the sampled trajectory with the lowest total cost. However, the cost map generated by convolutional neural networks imposes a significant computational burden and fails to meet real-time requirements. Additionally, planning in high-speed scenarios necessitates a larger map range and an excessively large grid size results in reduced planning accuracy. At the same time, a considerable portion of the large-scale grid behind the car or in unreachable areas is also predicted, resulting in a waste of computing resources. Consequently, this method faces a trade-off between computation time, map range, and grid size. Moreover, the pure cost value only provides information about spatiotemporal location, without considering higher-order motion information. For instance, the cost of driving to the roadside and driving along the roadside should differ, and the cost map cannot convey information about the road's

speed limit.

To address these challenges, we propose the *Velocity Fields* (VF), which comprises two novel key designs. First, to overcome the computational tradeoff, we propose the concept of implicit maps implemented based on the attention mechanism [3]. In our method, the driving context information is encoded as key-value pairs, while the trajectory sampling position is encoded as a query to obtain the driving cost at that position. This approach avoids explicitly decoding the latent variable into a rasterized map and outputting the cost value of irrelevant positions, resulting in higher computational efficiency and no trade-off between grid range and size. Second, similar to the relationship between the occupancy map [4] and occupancy flow [5], we replace the original cost values with the velocity vectors (Fig. 1 (c)), which introduces higher-order motion information. The traveling cost is estimated by computing the difference between the trajectory velocity and the velocity priors. We validate our method on a dataset that records real-world scenarios.

Our contributions are mainly three folds:

- 1) We explore a novel interpretable vectorized driving local map representation method, termed *Velocity Field* (VF), which boosts the planning performance in a straightforward and efficient manner.
- 2) We develop an efficient iterative trajectory optimizer that is seamlessly compatible with the proposed map representation method, enabling both the training and inference process.
- 3) We deploy *Velocity Field* and iterative optimization-based planners in the recorded scenarios from the real world in closed-loop form, demonstrating the human similarity and safety improvements achieved by our proposed method.

II. RELATED WORK

A. Environment Feature Extraction

Due to advancements in feature extraction using Deep Neural Networks (DNN), numerous learning-based planning approaches have been proposed [6], [7]. These approaches take rasterized maps and vehicle history trajectories as input and output different hypotheses assigning probabilities to each trajectory. Some alternative methods [8], [9] encode contextual information in vector and graph formats, which have proven to be more powerful due to their enhanced efficiency in context representation. Furthermore, these methods employ attention mechanisms or graph convolution techniques to aggregate information and learn latent interaction models, enabling the planner to focus more on the most relevant information. Jie *et al.* [10] proved that emphasizing domain knowledge by explicitly broadcasting map elements can improve performance on related aspects like lane selection. These feature extraction and processing methods inspired the encoder design of our approach.

B. Representation of Local Map Information

The local map differs from the global map as it expresses scene information in the presence of time-dependent traffic

participants and rules. In the past few decades, the concept of occupancy grid maps [4] and configuration space had been widely used to empower planning algorithms of autonomous driving. However, this method only enables the agent to have basic obstacle avoidance capabilities and cannot meet the requirements of following traffic regulations on urban roads. HD maps [11] offer semantic information that is essential for urban planning, including lanes, stop lines, and traffic signs. They have been widely used in rule-based planning methods. Our method also makes good use of the semantic information and integrated them with learning-based methods by rule check. Learning-based research tended to improve their reliability by constraining resulting trajectories using occupancy maps [12], [13] or by calculating distances from the reference line [14]. NMP [2] explored the use of neural networks to generate spatiotemporal cost maps using deconvolution modules. However, cost map-based methods can only offer first-order planning information which is lack of direction and speed guidance.

Vector Field is an informative local map representation as it can offer more robust guidance for path following [15], [16]. However, it has only been applied to the control problem of tracking reference lines. In contrast, we combined it with deep neural networks to deal with complex road conditions. Recently, the implicit occupancy flow field [17] is proposed to predict occupied space regarding time by cross attention which is similar to ours. They are primarily concerned with motion prediction and its accuracy, whereas we are concerned with the construction of planning guidance based on scenario information.

C. Inverse Optimal Control

Inverse Optimal Control (IOC) is to learn the parameterized strategy to deal with objects in traffic scenes during driving from demonstration data [18]. Levine *et al.* [19] adopted this method to regress the parameters of the planning strategy. Previous works [2], [14] have integrated end-to-end learning with a sampling-based planner, achieved either by estimating a cost volume or predicting diverse future trajectories of other agents. However, their trajectory samples use parameterized curves or clustered trajectory logs, resulting in sparse data that cannot meet the needs of the planner. Furthermore, the reproducibility of their results is limited due to reliance on private datasets, which restricts further validation and application of the methods. DIPP [20] is the first to combine numerical optimization approaches with regressive model parameters by ensuring the trajectory optimization process is differentiable, achieving state-of-the-art planning and prediction accuracy.

III. METHODOLOGY

A. Problem Formulation

The objective of this task is to generate a set of future trajectory points for the ego vehicle, denoted as $\mathbf{P} = [\mathbf{p}^1, \dots, \mathbf{p}^T]$, over a short time period T , given the historical tracking data of other agents h_a and the ego vehicle h_e , as well as the map information of the current time \mathcal{M} , which

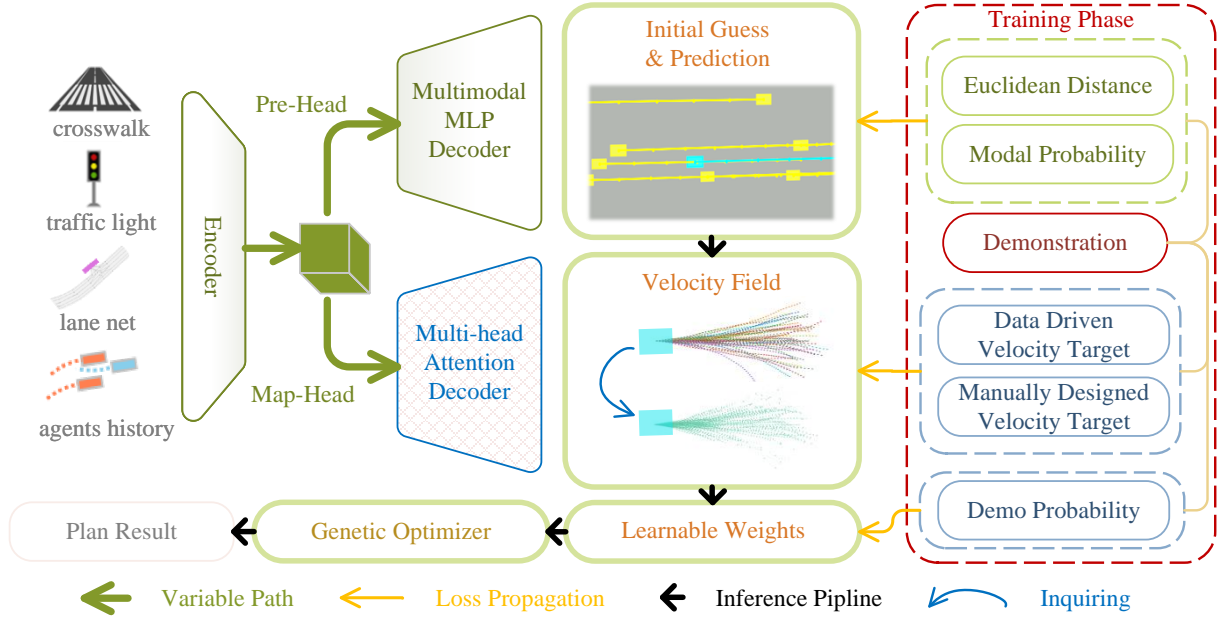


Fig. 2. The diagram presents our proposed framework for velocity field generation and planning modules, along with their training process. The **green arrows** represent the transmission of latent variables. Reference lines, map elements, ego and agent motion, and geometry are encoded using MLP/GRU modules. Global attention is employed to model the interaction between objects. The multi-modal MLP decoder generates initial guesses for the ego vehicle and predictions for other agents. The **orange arrows** indicate the relationship between loss and each module: expert demonstrations provide supervisory signals to model parameters through loss functions, such as distance measures, selection probabilities, and velocity targets. The **black arrows** represent the planning process: the iterative trajectory optimizer samples around the initial guess; calls the **inquiry function** to obtain speed information at each point of **ego vehicle** trajectory candidates; calculates the cost of each track through weighted summation; select the best n trajectories for the next iteration; and after a certain number of iterations; selects the one with minimum cost as the final output trajectory.

includes the reference lane m_{ref} , traffic light status m_{tl} , and static obstacles m_{ob} . The driving context is represented by $\mathcal{S} = (\mathbf{h}_a, \mathbf{h}_e, \mathcal{M})$, and our model aims to establish a mapping from the driving context to trajectory points $\mathbf{P} = \mathcal{F}(\mathcal{S})$. The overall method is illustrated in Fig. 2.

B. Driving Context Encoding

Similar to Vectornet [8], we implement a graph neural network to encode vectorized context information for the prediction module. Both the T time step ego-vehicle history $\mathbf{h}_e \in \mathbb{R}^{T \times [x, y, yaw, \dot{x}, \dot{y}]}$ and N_a surrounding vehicles $\mathbf{h}_a \in \mathbb{R}^{N_a \times T \times [x, y, yaw, \dot{x}, \dot{y}, type]}$ features are concatenated together and embedded by a Gated Recurrent Unit (GRU) to encode the time-dependent information. Subsequently, the features extracted in a 256-dimensional space are processed by a multi-layer perceptron (MLP). Map elements like piecewise lanes and crosswalks polyline are initially directly encoded by MLP. All the 256-dimensional encoded features are concatenated in the first dimension and aggregated by a global multi-head attention network (GAT) to obtain the vehicle-to-vehicle and vehicle-to-context relationships. The overall scenario context embedding is symbolized as \mathcal{S} .

This module generates predicted future trajectories of neighboring agents and an initial planning guess for the ego vehicle. Trajectory replays from the dataset directly serve as supervisory signals by computing the smoothed L1 loss, thereby guiding the trajectory optimization process.

C. Iterative Gaussian Sampling Trajectory Optimizer

During the training and inference process, we adopted an iterative Gaussian sampling-based planner to enhance sampling efficiency and improve sampling accuracy. The optimization process is similar to STOMP [21]. In our work, the sampler performs Gaussian sampling regarding control variables including acceleration and steering (a, s) , which is obtained by differentiating the initial guess. It selects the best k samples as new means and resamples until the diagnosed iter limit. Three categories of trajectories constitute the samples in the first loop: a control variable probabilistic grid sampler, a lattice state sampler [22], and the initial guess based on vanilla imitation learning. The sampling variance for acceleration and steering is controlled by two independent hyperparameters (σ_a, σ_s) and sampled independently.

It is important to note that the disturbance in the first iteration is time-constant, while in the subsequent iterations, it is time-dependent with decreasing variance. The first loop aims to ensure that the most feasible trajectories are explored, while the following iterations optimize the best choice.

D. Implicit Velocity Field

Implicit Velocity Field is a module that maps position (x, y) and time stamp t queries to advised velocity vectors $\mathbf{v} = f(x, y, t | \mathcal{S})$ regarding the scenario context embedding. The attention mechanism computes the distance between query (Q) and key (K) as a weight, and multiplies it with the value (V), as depicted in Fig.3. This approach effectively

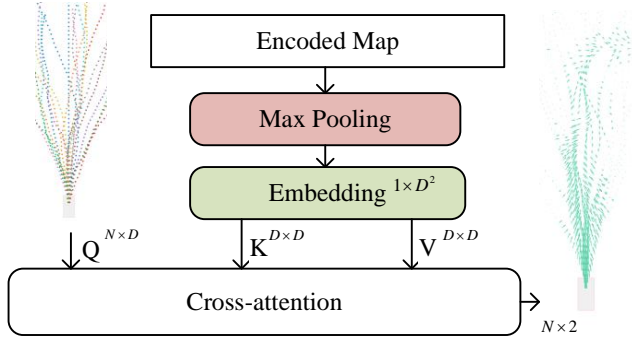


Fig. 3. The planning trajectories sampled around the initial guess are encoded as the query. The encoded map representation is reshaped into D embeddings with the same dimension as the query. The multi-head cross-attention module then outputs 2-dimensional vectors representing the recommended velocity at each query point, effectively guiding the trajectory optimization process.

captures the relationships and interactions among various elements in the driving context.

We incorporate the querying framework into our method. Positions with time embedding $(x, y, t, \sin(t), \cos(t))$ serve as queries for velocity scale in orthogonal directions (\dot{x}, \dot{y}) . Linear layers are implemented to embed tokens and generate velocity vectors before and after the attention module, effectively capturing the dynamics of the driving context and generating appropriate guidance for trajectory planning.

The velocity vectors are generated regarding to the trajectory samples $\mathcal{T}_{sample} = [\mathcal{T}_1, \dots, \mathcal{T}_N]$ by equation

$$\mathcal{V}_{p,M}^{t,n} = \mathcal{M}(\mathbf{p}_{\mathcal{T}}^{t,n} | \mathcal{S}),$$

where \mathcal{M} is the velocity inquiry function, $\mathbf{p}_{\mathcal{T}}^{t,n}$ is the position of number n trajectory point at time t , and $\mathcal{V}_{p,M}^{t,n}$ is the velocity vector we get from the implicit *Velocity Field* module. The velocity of the nearest n samples is considered to be an acceptable velocity value. Each velocity imitation loss is multiplied by an exponential discount regarding L2 distance between $[x, y, yaw]$ of the demonstration trajectory and the sampled location by

$$\mathcal{L}_{imit} = \frac{1}{Z} \sum_{n=0}^N \sum_{t=0}^T e^{-\frac{\|\mathbf{p}_{\mathcal{T}}^{t,n} - \mathbf{p}_{\mathcal{T}_e}^t\|_2}{2}} (\mathcal{V}_{p,M}^{t,n} - \mathcal{V}_{p,\mathcal{T}}^{t,n}).$$

We introduce a velocity correction loss to assign the appropriate velocity to each position. It is assumed that the velocity at the current time step should be capable of guiding the ego vehicle along the demonstration trajectory point in the subsequent time step. This design is to ensure the planning remains consistent with the desired trajectory while maintaining smoothness and safeness. The correction loss is defined by

$$\hat{\mathcal{V}}_{p,\mathcal{T}}^{t,n} = (\mathbf{p}_{\mathcal{T}_e}^{t+1,n} - \mathbf{p}_{\mathcal{T}}^{t,n}) / dt,$$

$$\mathcal{L}_{correct} = \frac{1}{Z} \sum_{n=0}^N \sum_{t=0}^{T-1} e^{-\frac{\|\mathbf{p}_{\mathcal{T}}^{t,n} - \mathbf{p}_{\mathcal{T}_e}^t\|_2}{2}} \|\hat{\mathcal{V}}_{p,\mathcal{T}}^{t,n} - \mathcal{V}_{p,M}^{t,n}\|_2.$$

The *Velocity Field* construction loss is defined as

$$\mathcal{L}_{VF} = \mathcal{L}_{imit} + \mathcal{L}_{correct}.$$

E. Traveling Cost Estimation

The traveling cost estimation function is constructed with Lagrangian items, including acceleration, jerk, steering, steering change, and the velocity difference \mathcal{V}_{diff} between the sample velocity and the map-suggested velocities. These components are combined using a weighted sum with learnable coefficients \mathbf{w}_c , enabling the optimization process to efficiently adapt and respond to various driving scenarios. The raw measurements vector is

$$\mathcal{D} = \sum_{t=0}^T [\ddot{x}_t^2, \ddot{x}_t^2, \dot{H}_t^2, \dot{H}_t^2, \mathcal{V}_{diff}^2],$$

and target function can be mathematically represented as

$$\mathcal{C}_{\mathcal{T}} = \mathcal{D} \mathbf{w}_c^T.$$

Different from NMP [2], which directly maps Average Distance Error (ADE) between expert trajectory and negative samples to traveling cost to smooth the cost value of negative samples, we affine the average distance to probabilistic space. The selection loss calculates the Cross Entropy (CE) of cost distribution and distance distribution of sampling trajectory set \mathcal{T}_s by

$$\mathcal{P}(\text{ADE}) = \text{Softmax}(1 - \eta(\|\mathcal{T}_s - \mathcal{T}_e\|_2)),$$

$$\mathcal{P}(\mathcal{C}_{\mathcal{T}_{samp}}) = \text{Softmax}(1 - \eta(\mathcal{C}_{\mathcal{T}_{samp}})),$$

$$\mathcal{L}_{sele} = \text{CE}(\mathcal{P}(\mathcal{C}_{\mathcal{T}_s}), \mathcal{P}(\text{ADE})),$$

where η is the normalization function along sampled candidate trajectories. Please note that not all the samples are taken into loss calculation, only 20 samples with lower cost are considered.

In addition to \mathcal{L}_{VF} and \mathcal{L}_{sele} , we introduce a multi-modal Imitation Learning planning and multi-agent prediction head to generate initial guesses and provide multi-modality information, respectively. For the initial guessing and prediction head, the loss is defined as follows:

$$\mathcal{L}_{IL} = \mathcal{L}_{ADE}^{plan} + \mathcal{L}_{FDE}^{plan} + \mathcal{L}_{ADE}^{pre} + \mathcal{L}_{modal},$$

where \mathcal{L}_{modal} is the cross-entropy loss of modal selection. The modal with the minimum summation of the plan and prediction error is expected to have the highest probability. Finally, the overall training loss is

$$\mathcal{L} = \mathcal{L}_{VF} + \mathcal{L}_{sele} + \mathcal{L}_{IL}.$$

IV. EXPERIMENT

A. Implementation details

1) *Dataset*: Our experiments are conducted on the Waymo open motion Dataset [23], which contains 104k, 20s time horizon, and real-world driving samples, collected on a complex urban route. HD maps and annotations for traffic signals/participants are provided at 10 Hz. 1000 packages with 100 scenarios in each package are provided. The 0 to 699 and 700 to 899 are segmented as training and validating datasets respectively. The scenarios are processed into 7-second object tracks. The training set consists 641943 tracks and validating set consists 182731 tracks. For each track,

TABLE I: OPEN-LOOP COMPARISON

Methods	Collision↓	Off Route↓	Traffic Light↓	Acc↓	Jerk↓	Prediction ADE↓	Prediction FDE↓	Plan L2@1s↓	Plan L2@3s↓	Plan L2@5s↓
Human	0.12%	0.70%	2.38%	0.6546	3.2496	0.0000	0.0000	0.0000	0.0000	0.0000
IL	1.44%	1.26%	1.44%	0.5794	2.5236	0.6893	1.7352	0.0920	0.7191	2.1360
DIPP [20]	6.70%	5.08%	1.49%	2.4164	27.9553	0.6547	3.2497	0.3144	1.4119	3.5733
EULA	9.65%	1.69%	1.36%	0.4470	0.3350	0.7406	1.8617	0.2305	1.1124	2.7648
CF	6.26%	0.32%	1.61%	0.8026	4.5039	0.7379	1.8579	0.4014	3.0564	8.2568
VF(ours)	8.01%	1.65%	1.41%	0.4850	0.2464	0.7071	1.7555	0.1371	0.8743	2.4642

TABLE II: CLOSED-LOOP COMPARISON

Methods	Collision↓	Off Route↓	Traffic Light↓	Progress↑	Acc↓	Jerk↓	Lat.Acc↓	Plan L2@3s↓	Plan L2@5s↓	Plan L2@10s↓
IL	40.00%	15.00%	1.00%	28.9308	1.7357	3.5291	0.2030	5.9404	10.7390	25.5545
DIPP	9.00%	0.00%	5.00%	69.7017	0.8945	3.4976	1.0862	2.4340	4.9987	11.0548
EULA	11.50%	4.00%	3.00%	78.3942	0.7345	5.6692	0.0961	2.3328	4.5252	9.4676
CF	21.00%	1.00%	0.00%	49.0182	0.5945	4.1452	0.0650	2.1357	4.5088	10.8249
VF	6.00%	0.00%	1.00%	55.0490	0.8580	7.7434	0.1101	1.9397	3.4757	8.9564

the first 2 seconds are considered as track history and the following 5 seconds are expert planning track and prediction ground truth. The first scenarios in files 900 to 999 are for closed-loop testing and all the scenarios in those files are for open-loop testing.

$$\mathcal{U}_{his}^{aug} = \mathcal{U}_{his} + \mathcal{N}(0, \varepsilon \cdot \mathbf{u}_{lim}) \quad (1)$$

$$\mathcal{X}_{his}^{aug} = \text{BicycleModel}(\mathcal{U}_{his}^{aug}, \mathcal{X}_{his}^{t=0}) \quad (2)$$

To reduce the domain shift problem in imitation learning, we propose a novel approach that leverages a time-dependent Gaussian distribution to augment the control variables of the driving history. Specifically, we apply equations (1) and (2) to introduce variability to the control inputs, while leaving the future trajectory unchanged. Data augmentation is implemented in all the experiments without special statements.

2) *Training*: Training with AdamW [24] optimizer and learning rate $1e-4$ for 20 epochs are conducted on a server equipped with $4 \times \text{RTX3090}$ GPU and 2×48 threads Intel(R) Xeon(R) Gold 5318S CPU @2.10GHz. The iterative sampling optimizer conducts 3 iterations in the training process and 10 iterations in validating process. The best 10 samples are selected as parents in the iterative sampling process. A two-stage supervised learning process is conducted. We first train the prediction model from all the vehicles for 2 epochs. Then the map parameter and cost function training process is conducted by imitating the behavior demo of the ego vehicle.

3) *Evaluation*: We compare our model and other baselines on the dataset with common metrics. Average Distance Error(ADE)(m), and Final Distance Error(FDE)(m) are introduced to illustrate the ability to **imitate** expert behavior. Collision Rate(CR), Off-Road Rate(ORR), and Traffic Light Violation(TLV), are **safety** measurements. Acceleration (Acc)(m/s^2), Jerk(m/s^3) measures the **comfortness**. L2 distance at typical time steps ($L2@Ns$) is introduced to reveal more accurate distance errors.

B. Baselines

Imitation Learning (IL), where the input is vectorized context [8] and directly outputs multi-modal future ego plan controls and trajectory of other agents.

Differentiable Integrated Motion Prediction and Planning (DIPP) is inverse optimal control based planning method. Where the IL model is implemented to offer initial guess and trajectory prediction of other agents. Euclidean distance to on-road objects and trajectory smoothness are weighted sums to estimate driving costs [20]. Please note that data augmentation is not applicable to this method.

Sampling Based DIPP (EULA) also measures Euclidean distances using the same cost function as DIPP but implemented with our proposed iterative sampling planner in both the training and evaluating processes.

Cost Field (CF) use the same framework as our proposed Velocity Field, but the vector outputs are summed to be scalar to directly represent the driving cost of the inquired point.

Velocity Field (VF) our proposed method, the implementing details are described in Section III.

C. Open-loop Comparison

Table I presents the open-loop results of the methods described above. The first row labeled **Human** indicates that the data in the simulation system has some noise and inaccuracies, despite being roughly accurate. In general, all deep neural network-based methods, including IL, are able to accurately imitate the behavior of human drivers, demonstrating the effectiveness of deep learning in pattern recognition. Comparing DIPP and EULA, we observe a reduction in imitation metrics, indicating that our iterative sampling planner can find low-cost trajectories that closely resemble the expert demonstrations. By comparing the CF and VF metrics, we find that incorporating the prior velocity vector can improve the accuracy of the cost calculation and lead to more precise results. Overall, these open-loop results suggest that our proposed method can achieve comparable

or better performance than the state-of-the-art baselines in terms of imitating human driving behavior, safeness, and comfortness.

D. Closed-loop Comparison

Table II presents the closed-loop results, which provide a more realistic assessment of the model's ability to handle domain shift and generalize to real-world driving scenarios. Despite the use of data augmentation, the deep neural network (DNN) planner struggles to cope with complex dynamic driving environments. In contrast, DIPP leverages manually designed rules to optimize the planning strategy of the model, resulting in significant improvements in planning security. By comparing DIPP, and EULA, we found that the planning module used in EULA is not as effective as Gauss-Newton for finding the optimal trajectory. But it still outperforms the DNN-based methods in terms of safety and similarity to human drivers and achieves comparable results as DIPP. For the CF method, the worse result in collision rate, progress and similarity compared with VF proves its limited capability. Because it can only provide first-order information for the downstream optimization module. The VF method effectively uses expert data to form an information-rich local map, avoiding inductive bias due to manual design and various traffic information interaction modes. As a result, VF achieves better results in terms of safety and imitation ability.

E. Operation Time

Operation time evaluation is conducted on a PC equipped with Intel 12900K and NVIDIA RTX3080Ti. The average operation time for generating a planning result is 0.048s (Min. 0.017, Max. 0.111). The operating time meets the real-time requirement.

V. CONCLUSION

In this work, we proved that *Velocity Field* is an informative way to offer traveling costs for local path planning, and demonstrate the effectiveness of the iterative sampling planner to generate safe trajectories by experiments. Our method significantly improves the planning performance compared to the baseline DIPP method. Specifically, it reduces the probability of collision by 33.3%, the probability of running a red light by 80%, and achieves the highest improvement of 43.81% in similarity with human drivers. Overall, our approach offers a promising solution for improving the planning performance of autonomous driving systems and enhancing their ability to imitate human driving behavior.

REFERENCES

- [1] O. Scheel, L. Bergamini, M. Wolczyk, B. Osiński, and P. Ondruska, "Urban driver: Learning to drive from real-world demonstrations using policy gradients," in *Conf. Rob. Learning*. PMLR, 2022, pp. 718–728.
- [2] W. Zeng, W. Luo, S. Suo, A. Sadat, B. Yang, S. Casas, and R. Urtasun, "End-to-end interpretable neural motion planner," in *Proc. of the IEEE/CVF Conference on Computer Vision and Pattern Recognition*, 2019, pp. 8660–8669.
- [3] A. Vaswani, N. Shazeer, N. Parmar, J. Uszkoreit, L. Jones, A. N. Gomez, Ł. Kaiser, and I. Polosukhin, "Attention is all you need," *Advances in neural information processing systems*, vol. 30, 2017.
- [4] H. Moravec and A. Elfes, "High resolution maps from wide angle sonar," in *Proceedings. 1985 IEEE International Conference on Robotics and Automation*, vol. 2, 1985, pp. 116–121.
- [5] R. Mahjourian, J. Kim, Y. Chai, M. Tan, B. Sapp, and D. Anguelov, "Occupancy flow fields for motion forecasting in autonomous driving," *IEEE Robotics and Automation Letters*, vol. 7, no. 2, pp. 5639–5646, 2022.
- [6] T. Phan-Minh, E. C. Grigore, F. A. Boulton, O. Beijbom, and E. M. Wolff, "Covernet: Multimodal behavior prediction using trajectory sets," *CoRR*, vol. abs/1911.10298, 2019. [Online]. Available: <http://arxiv.org/abs/1911.10298>
- [7] M. Bansal, A. Krizhevsky, and A. Ogale, "ChauffeurNet: Learning to drive by imitating the best and synthesizing the worst," in *Rob. Sci. Systems*, Freiburg/Breisgau, Germany, June 2019.
- [8] J. Gao, C. Sun, H. Zhao, Y. Shen, D. Anguelov, C. Li, and C. Schmid, "Vectornet: Encoding HD maps and agent dynamics from vectorized representation," in *Proc. of the IEEE/CVF Conference on Computer Vision and Pattern Recognition*, 2020, pp. 11 525–11 533.
- [9] N. Deo, E. Wolff, and O. Beijbom, "Multimodal trajectory prediction conditioned on lane-graph traversals," in *5th Annual Conference on Robot Learning*, 2021.
- [10] J. Cheng, R. Xin, S. Wang, and M. Liu, "Mnpn: Multi-policy neural planner for urban driving," in *IEEE/RSJ Int. Conf. Intell. Rob. Sys. (IROS)*. IEEE, 2022.
- [11] R. Liu, J. Wang, and B. Zhang, "High definition map for automated driving: Overview and analysis," *The Journal of Navigation*, vol. 73, no. 2, pp. 324–341, 2020.
- [12] H. Song, D. Luan, W. Ding, M. Y. Wang, and Q. Chen, "Learning to predict vehicle trajectories with model-based planning," in *5th Annual Conference on Robot Learning*, 2021.
- [13] D. Zhu, M. Zahran, L. E. Li, and M. Elhoseiny, "Motion forecasting with unlikelihood training in continuous space," in *Proceedings of the 5th Conference on Robot Learning*, ser. Proceedings of Machine Learning Research, A. Faust, D. Hsu, and G. Neumann, Eds., vol. 164. PMLR, 08–11 Nov 2022, pp. 1003–1012. [Online]. Available: <https://proceedings.mlr.press/v164/zhu22a.html>
- [14] S. Casas, A. Sadat, and R. Urtasun, "Mp3: A unified model to map, perceive, predict and plan," in *Proc. of the IEEE/CVF Conference on Computer Vision and Pattern Recognition*, 2021, pp. 14 403–14 412.
- [15] D. R. Nelson, D. B. Barber, T. W. McLain, and R. W. Beard, "Vector field path following for miniature air vehicles," *IEEE Transactions on Robotics*, vol. 23, no. 3, pp. 519–529, 2007.
- [16] D. A. Lawrence, E. W. Frew, and W. J. Pisano, "Lyapunov vector fields for autonomous unmanned aircraft flight control," *Journal of Guidance, Control, and Dynamics*, vol. 31, no. 5, pp. 1220–1229, 2008.
- [17] B. Agro, Q. Sykora, S. Casas, and R. Urtasun, "Implicit occupancy flow fields for perception and prediction in self-driving," in *Proceedings of the IEEE/CVF Conference on Computer Vision and Pattern Recognition*, 2023, pp. 1379–1388.
- [18] F. Yaman, V. G. Yakhno, and R. Potthast, "A survey on inverse problems for applied sciences," *Mathematical problems in engineering*, vol. 2013, 2013.
- [19] S. Levine and V. Koltun, "Continuous inverse optimal control with locally optimal examples," *arXiv preprint arXiv:1206.4617*, 2012.
- [20] Z. Huang, H. Liu, J. Wu, and C. Lv, "Differentiable integrated motion prediction and planning with learnable cost function for autonomous driving," *arXiv preprint arXiv:2207.10422*, 2022.
- [21] M. Kalakrishnan, S. Chitta, E. Theodorou, P. Pastor, and S. Schaal, "Stomp: Stochastic trajectory optimization for motion planning," in *2011 IEEE International Conference on Robotics and Automation*, 2011, pp. 4569–4574.
- [22] M. McNaughton, C. Urmson, J. M. Dolan, and J.-W. Lee, "Motion planning for autonomous driving with a conformal spatiotemporal lattice," in *2011 IEEE International Conference on Robotics and Automation*. IEEE, 2011, pp. 4889–4895.
- [23] S. Ettinger, S. Cheng, B. Caine, C. Liu, H. Zhao, S. Pradhan, Y. Chai, B. Sapp, C. R. Qi, Y. Zhou, *et al.*, "Large scale interactive motion forecasting for autonomous driving: The waymo open motion dataset," in *Proc. IEEE/CVF Conf. Comput. Vis. Pattern Recognit. (CVPR)*, 2021, pp. 9710–9719.
- [24] I. Loshchilov and F. Hutter, "Decoupled weight decay regularization," in *International Conference on Learning Representations*, 2018.